Asian Journal of Chemistry; Vol. 37, No. 3 (2025), 737-744

ASIAN JOURNAL OF CHEMISTRY

https://doi.org/10.14233/ajchem.2025.33334

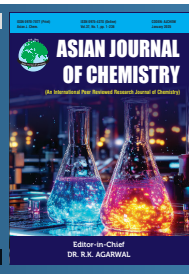

Synthesis, *in silico* ADME, Molecular Docking and *in vitro* Cytotoxicity Evaluation of Indolin-2-one linked Stilbene Derivatives

DIMPLE PIRGAL[1,2,*], SUBHAS S. KARKI[1,2,†], SUJEET KUMAR[3,†] and BASAVRAJ METIKURKI[3]

[1]Department of Pharmaceutical Chemistry, KLE College of Pharmacy, 2nd Block, Rajajinagar, Bengaluru-560010, India
[2]Dr. Prabhakar B. Kore Basic Science Research Centre (Off Campus), KLE College of Pharmacy, 2nd Block, Rajajinagar, Bengaluru-560010, India
[3]Department of Pharmaceutical Chemistry, Nitte College of Pharmaceutical Sciences, Nitte (Deemed to be University), Govindapura, Gollahalli, Yelahanka, Bengaluru-560064, India
†Authors contributed equally.

*Corresponding author: E-mail: dimplepirgal@gmail.com

Received: 7 January 2024; *Accepted*: 25 February 2025; *Published online*: 28 February 2025; AJC-21932

Considering the potential of stilbene derivatives as biologically active frameworks in cancer research, the synthesis of several indole-2-one linked stilbenes was proposed as evaluate their cytotoxic effects on cancer cells. To develop some indole-2-one linked stilbene analogs as lead molecule against cancer, novel indole-2-one linked derivatives (**BK 1-11**) were synthesized by reacting 4-formyl-*trans*-stilbene with 2-oxindole in methanol. The structural characterizations were performed by FTIR, NMR and mass techniques. Molecular docking was performed on the Janus kinase 2 (JAK2) receptor (Pdb ID: 4Z32), with binding energies expressed in kcal/mol. All the synthesized compounds were screened for their cytotoxicity against MCF, HCT116 and HeLa cells taking 5-fluorouracil (5-FU) and resveratrol as reference. Among tested derivatives, compound **BK-6** was found to be most potent against all the three cell lines with IC_{50} of 48-64 µM and 49.92% cell viability after 72 h of treatment. A low to moderate aqueous solubility was predicted by Swiss-ADME web-tool. The docking score and cytotoxicity data suggest compound **BK-6** as a potential molecule against MCF cancer cells. However, further biological studies require to support the cytotoxicity and *in silico* results.

Keywords: Stilbene, Indole, Cytotoxicity, Cell lines, JAK-2.

INTRODUCTION

Cancer is accounting for nearly 10 million deaths in 2022 with an estimated 30 million new cases by 2050 [1]. Regardless of the cause, it is essential to treat and eliminate cancer for the betterment of society. Chemotherapy, radiation, surgery, gene therapy and palliative care are commonly used to cure or control cancer. Despite all advancements, the survival rate in cancer is limited to 50% [2]. The surgery or radiation therapy is not sufficient alone and chemotherapy always comes with equal intensity of side effects. The simultaneous administration of multiple drugs causes severe toxicity.

Use of natural products to treat different chronic ailments is in practice since ancient times. These plants or their active constituents have attracted the scientific community for their health benefits and therapeutic values. For example, resveratrol, (3,4′,5-trihydroxy-*trans*-stilbene) is one among several. It is a non-flavonoid polyphenolic phytoalexin found in grapes, peanuts and berries, known for its cardio-protective, antioxidant, anti-aging and anti-inflammatory properties [3]. Studies report the use of resveratrol as an adjuvant in multidrug-resistant cancer. It sensitizes cancer cells towards the chemotherapeutic agents [4]. The stilbene derivatives like diethylstilbestrol and tamoxifen are clinically used to treat prostate and breast cancer, respectively [5]. The several other stilbene derivatives have also been reported in the literature for its anticancer properties [6-8].

Indole, (benzo[*b*]-pyrrole), is another naturally occurring moiety known for its synthetic versatility and outstanding pharmacological properties. The indole derivatives have been widely explored for their cytotoxic, antiviral, antimicrobial, anti-inflammatory and anti-hypertensive activities [9-12]. Tryptophan, vinblastine, vincristine, vallesiachotamine, reserpine,

ergotamine, *etc.*, are the few naturally occurring indole derivatives with medicinal values [13-18]. Considering the therapeutic potential of stilbene and indole nucleus, the present work is aimed to develop a potential stilbene based lead against cancer with minimal adverse effect.

EXPERIMENTAL

All chemicals used in this study were of LR grade, with some also being of AR grade and procured from Sigma-Aldrich and S.D. Fine Chemicals Ltd., India. Before use, the solvents and reagents were checked for purity. The melting points (m.p.) were recorded using a DBK digital melting point device and are reported without correction. FTIR spectra were obtained using a JASCO 460+ FTIR instrument. Proton NMR (^{1}H NMR) spectra were recorded on a Bruker Ultraspec AMX 400 instrument in DMSO-d_6 at 400 and 500 MHz. Mass spectrometry data were collected in positive ion mode using a Waters Xevo G2 XS-QTOF instrument (Milford, USA). Thin-layer chromatography (TLC) was performed on pre-coated silica gel plates from SD Fine Chemicals, Mumbai, India and R_f values were calculated accordingly.

General procedure for synthesis of (*Z*)-5-substituted-3-(4-((*E*)-styryl)benzylidene)indolin-2-one: Novel indolin-2-one linked stilbene derivatives (**BK 1-11**) were synthesized by adopting the procedures reported earlier [19,20]. In brief, equimolar quantity (0.001 M) of 2-oxindoles (**1**) and 4-formyl-*trans*-stilbene (**2**) were refluxed in methanol for 1 h in the presence of 0.5 mL of piperidine as catalyst. The progress of the reaction was monitored at different time intervals by TLC on silica-gel 60 plates, until a distinct spot of product was obtained. The precipitated mass was filtered and recrystallized from ethanol-DMF mixture in appropriate ratio (**Scheme-I**).

(*Z*)-3-(4-((*E*)-Styryl)benzylidene)indolin-2-one (BK-1): Yellow crystals, m.p.: 256-258 ºC, yield: 73%, R_f: 0.63. IR (KBr, ν_{max}, cm^{-1}): 3443, 3372, 3177, 3028, 2974, 2706, 1701, 1631, 1613, 1464, 1368. ^{1}H NMR (DMSO-d_6, 500 MHz) δ ppm: 6.90-6.86 (2H, m, Ar-H), 7.26-7.22 (1H, m, Ar-H), 7.33-7.29 (3H, m, Ar-H), 7.36 (s, 1H, Ar), 7.44-7.39 (m, 3H, Ar), 7.66-7.62 (4H, m, Ar-H), 7.76-7.76 (4H, m, Ar-H), 10.58 (1H, s, -NH). MS (ESI) of $C_{23}H_{17}NO$: *m/z* 324.18 (323.38).

(*Z*)-5-Fluoro-3-(4-((*E*)-styryl)benzylidene)indolin-2-one (BK-2): Orange crystals, m.p.: 281-283 ºC, yield: 59%, R_f: 0.53. IR (KBr, ν_{max}, cm^{-1}): 3246, 3112, 3029, 2928, 2787, 1739, 1645, 1617, 1480, 1375, 1186. ^{1}H NMR (DMSO-d_6, 500 MHz) δ ppm: 6.58-6.56 (1H, m, *J* = 7.6 Hz), 6.77-6.73 (1H, t, *J* = 16 Hz), 6.91-6.89 (2H, d, *J* = 8.0 Hz), 7.08-7.06 (2H, d, *J* = 6.4 Hz), 7.34-7.27 (4H, m, Ar-H), 7.46-7.36 (4H, m, Ar-H), 7.63 (3H, d, *J* = 7.2 Hz), 7.73 (2H, d, *J* = 6.8 Hz), 10.97 (1H, s, -NH), MS (ESI) of $C_{23}H_{16}FNO$: *m/z* 341.09 (341.37).

(*Z*)-5-Methyl-3-(4-((*E*)-styryl)benzylidene)indolin-2-one (BK-3): Orange crystals, m.p.: 273-274 ºC, yield: 71%, R_f: 0.59. IR (KBr, ν_{max}, cm^{-1}): 3172, 3082, 3026, 2913, 2859, 2815, 2711, 1701, 1614, 1598, 1447, 1416. ^{1}H NMR (DMSO-d_6, 500 MHz) δ ppm: 2.21 (3H, s, -CH_3), 6.81-6.79 (1H, d, *J* = 8.8 Hz), 7.09-7.07 (1H, d, *J* = 8.8 Hz), 7.35-7.31 (1H, t, *J* = 15.2 Hz), 7.47-7.39 (4H, m, Ar-H), 7.49-7.51 (1H, m, Ar-H), 7.58-7.60 (1H, m, Ar-H), 7.69-7.65 (2H, d, *J* = 7.6 Hz, Ar-H), 7.76-7.78 (4H, m, Ar-H), 10.52 (1H, s, -NH); MS (ESI) of $C_{24}H_{19}NO$: *m/z* 338.20 (337.41).

(*Z*)-5-Bromo-3-(4-((*E*)-styryl)benzylidene)indolin-2-one (BK-4): Orange crystals, m.p.: 287-289 ºC, yield: 72%, R_f: 0.56. IR (KBr, ν_{max}, cm^{-1}): 3377, 3163, 3058, 3024, 2864, 2748, 2703, 1699, 1548, 1450, 1383. ^{1}H NMR (DMSO-d_6, 500 MHz) δ ppm: 6.85-6.94 (1H, m, Ar-H), 7.26-7.36 (2H, m, Ar-H), 7.42-7.58 (4H, m, Ar-H), 7.67-7.69 (2H, m, Ar-H), 7.73-7.88 (4H, m, Ar-H), 7.94-7.97 (1H, m, Ar-H), 8.48-8.51 (1H, m, Ar-H), 10.78 (1H, s, -NH); MS (ESI) of $C_{23}H_{16}BrNO$: *m/z* 402.20 (402.05).

(*Z*)-5-Chloro-3-(4-((*E*)-styryl)benzylidene)indolin-2-one (BK-5): Orange crystals, m.p.: 290-292 ºC, yield: 63%, R_f: 0.54. IR (KBr, ν_{max}, cm^{-1}): 3160, 3063, 2858, 2730, 2703, 1700, 1625, 1597, 1508, 1448. ^{1}H NMR (DMSO-d_6, 500 MHz)

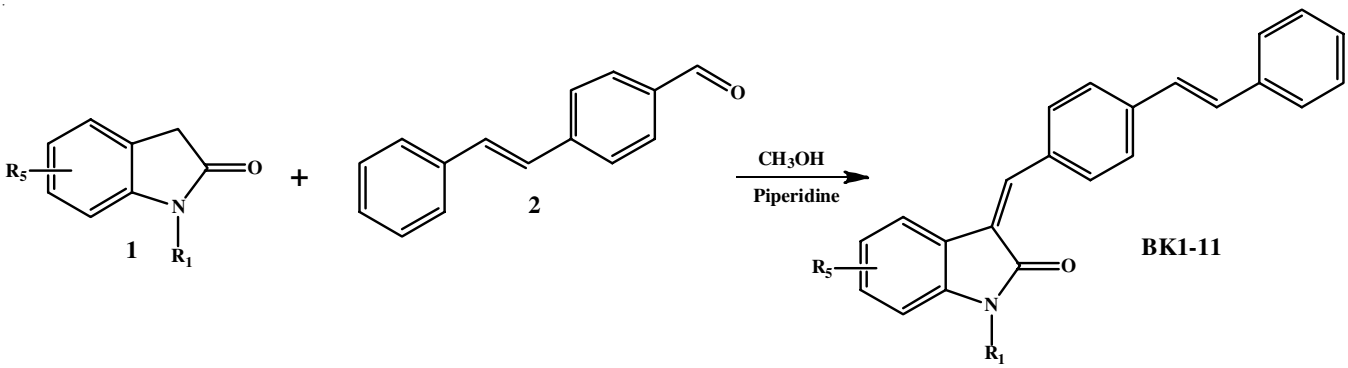

Code	R_1	R_5	Code	R_1	R_5
BK-1	-H	-H	**BK-7**	Benzyl	-Br
BK-2	-H	-F	**BK-8**	Benzyl	-Cl
BK-3	-H	-CH_3	**BK-9**	Benzyl	-NO_2
BK-4	-H	-Br	**BK-10**	4-Cl-benzyl	-H
BK-5	-H	-Cl	**BK-11**	4-NO_2-benzyl	-H
BK-6	-H	-NO_2			

Scheme-I: Synthesis of (*Z*)-3-(4-((*E*)-styryl)benzylidene)indolin-2-one (**BK 1-11**)

δ ppm: 6.91-6.94 (1H, d, *J* = 8.8 Hz), 7.40-7.38 (1H, t, *J* = 13.6 Hz), 7.55-7.45 (5H, m, Ar-H), 7.77-7.72 (4H, m, Ar-H), 7.81-7.88 (4H, m, Ar-H), 10.84 (1H, s, -NH); MS (ESI) of $C_{23}H_{16}ClNO$: *m/z* 357.22 (357.83).

(*Z*)-5-Nitro-3-(4-((*E*)-styryl)benzylidene)indolin-2-one (BK-6): Orange crystals, m.p.: 301-303 ºC, yield: 56%, R_f: 0.49. IR (KBr, ν_{max}, cm^{-1}): 3107, 3024, 2887, 2846, 2803, 1691, 1595, 1578, 1472, 1389. ^{1}H NMR (DMSO-d_6, 500 MHz) δ ppm: 6.96-6.84 (1H, d, *J* = 8.4 Hz), 7.48-7.38 (1H, t, *J* = 12.0 Hz), 7.56-7.53 (5H, m, Ar-H), 7.75-7.73 (4H, m, Ar-H), 7.83-7.77 (4H, m, Ar-H), 10.86 (1H, s, -NH). MS (ESI) of $C_{23}H_{16}N_2O_3$: *m/z* 368.13 (368.38)

(*Z*)-1-(4-Chlorobenzyl)-3-(4-((*E*)-styryl)benzylidene)-indolin-2-one (BK-7): Orange crystals, m.p.: 303-308 ºC, yield: 52%, R_f: 0.47. IR (KBr, ν_{max}, cm^{-1}): 3129, 3087, 3031, 2968, 2880, 2712, 1696, 1606, 1496, 1341. ^{1}H NMR (DMSO-d_6, 500 MHz) δ ppm: 5.08 (2H, s, -CH_2-), 6.76 (1H, m, Ar-H), 7.03-7.08 (1H, m, Ar-H), 7.18-7.20 (2H, m, Ar-H), 7.35-7.48 (4H, m, Ar-H), 7.64-7.74 (4H, m, Ar-H), 7.88-7.96 (3H, m, Ar-H). MS (ESI) of $C_{30}H_{22}BrNO$: *m/z* 493.03 (492.40).

(Z)-1-Benzyl-5-chloro-3-(4-((*E*)-styryl)benzylidene)-indolin-2-one (BK-8): Orange crystals, m.p.: 288-290 ºC, yield: 57%, R_f: 0.48. IR (KBr, ν_{max}, cm^{-1}): 3129, 3087, 3033, 2968, 2925, 1697, 1609, 1573, 1496, 1468, 1384. ^{1}H NMR (DMSO-d_6, 500 MHz) δ ppm: 4.99 (2H, s, -CH_2-), 6.65-6.64 (1H, d, *J* = 8.4 Hz), 6.86-6.82 (1H, t, *J* = 15.2 Hz), 7.03-7.01 (1H, d, *J* = 8.0 Hz), 7.10-7.07 (2H, d, *J* = 8.8 Hz), 7.16-7.15 (1H, d, *J* = 8.4 Hz), 7.31-7.38 (3H, m, Ar-H), 7.39-7.59 (7H, m, Ar-H), 7.61-7.65 (2H, m, *J* = 13.2 Hz), 7.73 (2H, d, *J* = 8.8 Hz); MS (ESI) of $C_{30}H_{22}ClNO$: *m/z* 448.08 (447.95).

(Z)-1-Benzyl-5-nitro-3-(4-((*E*)-styryl)benzylidene)-indolin-2-one (BK-9): Orange crystals, m.p.: 284-289 ºC, yield: 54%, R_f: 0.46. IR (KBr, ν_{max}, cm^{-1}): 3284, 3168, 3085, 3026, 2946, 2848, 1702, 1601, 1598, 1464, 1378. ^{1}H NMR (DMSO-d_6, 500 MHz) δ ppm: 4.89 (2H, s, -CH_2-), 6.75-6.71 (1H, d, *J* = 16.4 Hz), 6.90-6.83 (1H, t, Ar-H), 7.17-7.15 (1H, d, *J* = 8.4 Hz), 7.28-7.26 (2H, m, Ar-H), 7.32-7.29 (1H, d, *J* = 12.4 Hz), 7.37-7.31 (3H, m, Ar-H), 7.53-7.38 (7H, m, Ar-H), 7.59-7.55 (3H, m, Ar-H), 7.74-7.62 (2H, d, *J* = 13.2 Hz); MS (ESI) of $C_{30}H_{22}N_2O_3$: *m/z* 459.11 (458.50).

(Z)-1-(4-Chlorobenzyl)-3-(4-((*E*)-styryl)benzylidene)-indolin-2-one (BK-10): Orange crystals, m.p.: 288-292 ºC, yield: 57%, R_f: 0.48. IR (KBr, ν_{max}, cm^{-1}): 3219, 3085, 3046, 3028, 2923, 2864, 1704, 1605, 1598, 1468, 1387. ^{1}H NMR (DMSO-d_6, 500 MHz) δ ppm: 5.07 (2H, s, -CH_2), 6.76-6.74 (1H, d, *J* = 8 Hz), 7.07-7.05 (1H, d, *J* = 8 Hz), 7.20-7.17 (2H, d, J = 10.8 Hz), 7.40-7.27 (10H, m, Ar-H), 7.47-7.44 (4H, m, Ar-H), 7.74-7.63 (4H, m, Ar-H), 7.95-7.88 (2H, m, Ar-H); MS (ESI) of $C_{30}H_{22}ClNO$: *m/z* 447.08 (447.95).

(Z)-1-(4-Nitrobenzyl)-3-(4-((*E*)-styryl)benzylidene)-indolin-2-one (BK-11): Red crystals, m.p.: 287-289 ºC, yield: 56%, R_f: 0.47. IR (KBr, ν_{max}, cm^{-1}): 3184, 3096, 3036, 2946, 2850, 2724, 1704, 1601, 1548, 1458, 1361. ^{1}H NMR (DMSO-d_6, 500 MHz) δ ppm: 4.86 (2H, s, -CH_2), 6.65-6.63 (1H, d, *J* = 8.8 Hz), 6.85-6.81 (1H, t, *J* = 7.2 Hz), 7.03 -7.01 (1H, d, *J* = 8 Hz), 7.10-7.07 (2H, m, Ar-H), 7.17-7.15 (1H, d, *J* = 8.4 Hz), 7.27-7.32 (3H, m, Ar-H), 7.36-7.43 (7H, m, Ar-H), 7.46-7.65 (2H, m, Ar-H), 7.88 (2H, d, *J* = 8 Hz); MS (ESI) of $C_{30}H_{22}N_2O_3$: *m/z* 448.08 (458.50).

***In vitro* cytotoxicity studies:** The MTT test was used to assess the cytotoxicity of the synthsized compounds **BK 1-11** in accordance with reported method [21]. Briefly, 10,000 MCF7 (human breast cancer), HCT116 and Hela cells were seeded per well of 96-well plates, with a final volume of 100 µL per well. Different quantities of compounds **BK 1-11** (200, 100, 50, 25, 12.5 µM) were applied to the cells and then incubated for 24, 48 and 72 h. To prepare the MTT solution, dissolved 5 mg of MTT in 1 mL PBS and diluted the mixture with media to a working concentration of 0.5 mg/mL. Added 100 µL of 0.5 mg/mL MTT solution to each well. The cells underwent an additional 4 h of incubation at 37 ºC. Following the incubation phase, each well was treated with 100 mL of DMSO to facilitate the dissolution of the formazan and absorbance was recorded at 570 nm using a spectrophotometer. Data was represented as % viability using the formula given below:

$$\text{Viability (\%)} = \frac{\text{OD of sample} - \text{OD of blank}}{\text{OD of untreated} - \text{OD of blank}} \times 100 \quad (1)$$

The absorbance at 570 nm is proportional to the number of viable cells.

***In silico* studies**

Docking and molecular dynamics: Every stilbene derivative was docked into the tyrosine-protein kinase/Janus complex (Jak2 (kinase 2) receptors). PyRx software was used to create all of the ligands and the target and AutoDock Vina software was used to perform the docking experiment with the algorithm for Lamarckian genetics (LGA) [22,23]. The docking results visualizations were obtained using the Discovery studio software [24]. Using Avogadro (Version1.2.0), the 3D structures were created [25]. The MMFF94s force field was utilized to the minimize energy. The structure of the protein 4Z32 (JAK 2 receptor) was improved and adjusted to fix any structural anomalies [26]. Hydrogen atoms added to the protein structure and appropriate ionization states assigned based on the desired pH conditions. Water molecules and other hetero atoms removed before docking. The binding site analysis was performed using sitemap. The ADME and drug-likenesses were investigated using Swiss-ADME webserver [27,28].

A molecular dynamics (MD) simulation was performed on the docked complex of jak2 with 5-fluorouracil (5FU) and compound **BK-6** using OPLS4 force field [29]. The simulation was carried out for 100 ns under isothermal-isobaric (NPT) conditions at 300 K and 1.013 bar pressure. The solvent model used was TIP3P and the boundary was set to default with an orthorhombic box shape. The system volume was minimized and sodium (Na^+) and chloride (Cl^-) ions were added at 0.15 M concentration.

RESULTS AND DISCUSSION

Eleven indole linked stilbene analogs **BK 1-11** were synthesized by reacting substituted indolin-2-one and *E*-formyl stilbene in 40 mL methanol and 0.5 mL piperidine. The structural confirmation was performed with FTIR, NMR and mass

spectrometry. The indole -NH stretching peaks appeared between 3443-3107 cm^{-1} while the aromatic and aliphatic -CH stretching were observed in the range of 3112-3024 cm^{-1} and 2974-2803 cm^{-1}, respectively. Intense carbonyl (>C=O) stretching peaks appeared between 1739-1691 cm^{-1}. The -NO_2 stretching peaks in compounds **BK-6**, **9** and **11** appeared in the range of 1578-1548 and 1378-1361 cm^{-1}, while the peaks for -CH_3 bending in compound **BK-3** appeared at 1447 cm^{-1}. The -C=C-aromatic stretching appeared between 1614-1605 and 1472-1450 cm^{-1}. Further structural confirmation were done by ^{1}H NMR and mass spectrometry. The (-NH) protons of compounds **BK 1-6** appeared at δ ppm 10.97-10.59. Aromatic protons observed between 8.51-6.58 δ ppm. Peaks for -CH_2 protons appeared between 4.86-5.08 δ ppm for compounds **BK 7-11**. The methyl protons (-CH_3) of compound **BK-3** appeared at δ ppm 2.21. The *m/z* values were also found in close proximity with calculated mass of the molecule confirming their structure.

Cytotoxicity: Compound **BK-6** found to be most potent with IC_{50} of 48, 64 and 57 μM against MCF-7, HCT-116 and HeLa cell lines, respectively. A 50-100% viability was observed after MTT assay on MCF-7 cell lines. None of the compounds were found more potent than 5-fluorouracil (5-FU) and resveratrol (RSV). All the results are summarized in Tables 1 and 2.

TABLE-1
IC_{50} VALUE OF SYNTHESIZED DERIVATIVES (**BK1-11**) AND THE REFERENCE COMPOUNDS (5FU AND RSV)

Compound	IC_{50}* (μM)		
	MCF7	HCT116	HeLa
BK1	243	92	90
BK2	200	93	125
BK3	151	100	113
BK4	110	61	47
BK5	130	69	98
BK6	48	64	57
BK7	132	80	111
BK8	142	93	102
BK9	210	99	86
BK10	240	105	117
BK11	250	101	97
RSV	124	295	189
5FU	212	144	357

***In silico* analyses:** The drug-likeness properties of the synthesized compounds **BK 1-11** were evaluated using Lipinski, Ghose, Veber, Egan and Muegge filters. Molecule **BK-6** had shown zero violations while rest of the derivatives had shown two or more than two violations. All the molecules were poor to moderate water-soluble (ESoL: -5.44 to -7.84) with oral bioavailability of 0.55. The negative log Kp values by all molecules (-3.73 to -5.0) indicate moderate skin permeability. The physico-chemical properties of compounds **BK 1-11**, RSV and 5FU are summarized in Table-3 and Fig. 1.

All the molecules were docked against 4Z32 proteins with binding affinity of -4.4 to -7.8 kcal/mol, similar to reference drug RSV (-7.8 kcal/mol) and 5-FU (-6.4 kcal/mol) (Table-4). Molecule **BK-6** engaged in the hydrogen bond interactions with CYS 797, ASP 800 and LEU 718. The primary type of interactions observed was hydrophobic, indicating the intrinsic characteristics of compound. Compound **BK-6** aromatic ring participated in pi-pi interactions with amino acid LEU 718, LEU 844, ALA 743, VAL 726, MET 790 and LYS 745. The *para*-hydroxyl groups within resveratrol engaged in H-bond interactions with LEU 932. The hydrophobic pi-pi interactions were noted with VAL 863, LEU 855, ALA 880 and LEU 983. The 5-FU–NH and carbonyl oxygen interacted with amino acid LEU 932 (Fig. 2a-c).

The RMSD plot indicates that all simulations have reached a state of convergence, suggesting stable molecular dynamics behaviour. Specifically, the plot reveals that the RMSD values for both the *apo* and resveratrol simulations remain below 3.5 Å, indicating relatively minor deviations from their initial structures. However, for the compound **BK6** simulations, the RMSD values fall within the range of 3.5 Å to 4.5 Å, suggesting more significant structural fluctuations compared to *apo* and resveratrol. This observation implies that BK6 induce significant conformational changes in the protein structure during the simulation period (Fig. 3).

The RMSF plot reveals that the amino acid residues of the protein exhibit predominantly similar fluctuations, with only minor variations occurring in specific regions. Notably, in the 153-201 region, the RMSF was significant elevated for compound **BK6** compared to resveratrol. Resveratrol demonstrated the least RMSF, followed by compound **BK6**, whereas the RMSF values for *apo* was comparable in the 241 region. Moreover, the RMSF values were highest for the 273 and 297 regions in the *apo* form (Fig. 4).

Conclusion

Given the biological significance of stilbenes in cancer therapy, the present study focused on the stilbene moiety as a lead molecule. A series of indole-linked stilbene analogues **BK 1-11** were synthesized by reacting substituted indolin-2-ones with *E*-formyl stilbene. The synthesized compounds were characterized and screened for cytotoxicity using the MTT assay on MCF-7, HCT-116 and HeLa cells, with 5-fluorouracil (5-FU) as a positive control and resveratrol as a reference. Among

TABLE-2
% VIABILITY OF MCF7 CELL LINE AFTER TREATMENT WITH SYNTHESIZED DERIVATIVES AND THE REFERENCE COMPOUNDS (5FU AND RSV)

Conc. (μM)	**BK-1**	**BK-2**	**BK-3**	**BK-4**	**BK-5**	**BK-6**	**BK-7**	**BK-8**	**BK-9**	**BK-10**	**BK-11**	5FU	RSV
200	56.75	67.05	64.22	67.04	64.51	49.92	57.59	66.90	67.36	68.16	87.97	15.14	51.86
100	87.38	88.65	85.71	72.53	89.65	87.35	92.97	84.63	78.30	94.22	87.06	71.88	79.86
50	97.37	92.84	92.56	82.27	93.94	92.11	100.01	93.51	81.66	83.98	78.48	74.42	81.1
25	93.43	97.41	90.73	95.37	97.41	92.66	96.89	95.84	84.40	99.69	99.58	79.13	98.97
12.5	97.25	100.67	95.61	92.90	100.97	98.44	100.22	99.19	88.98	101.87	99.21	104.39	93.23
0	100	100	100	100	100	100	100	100	100	100	100	100	100

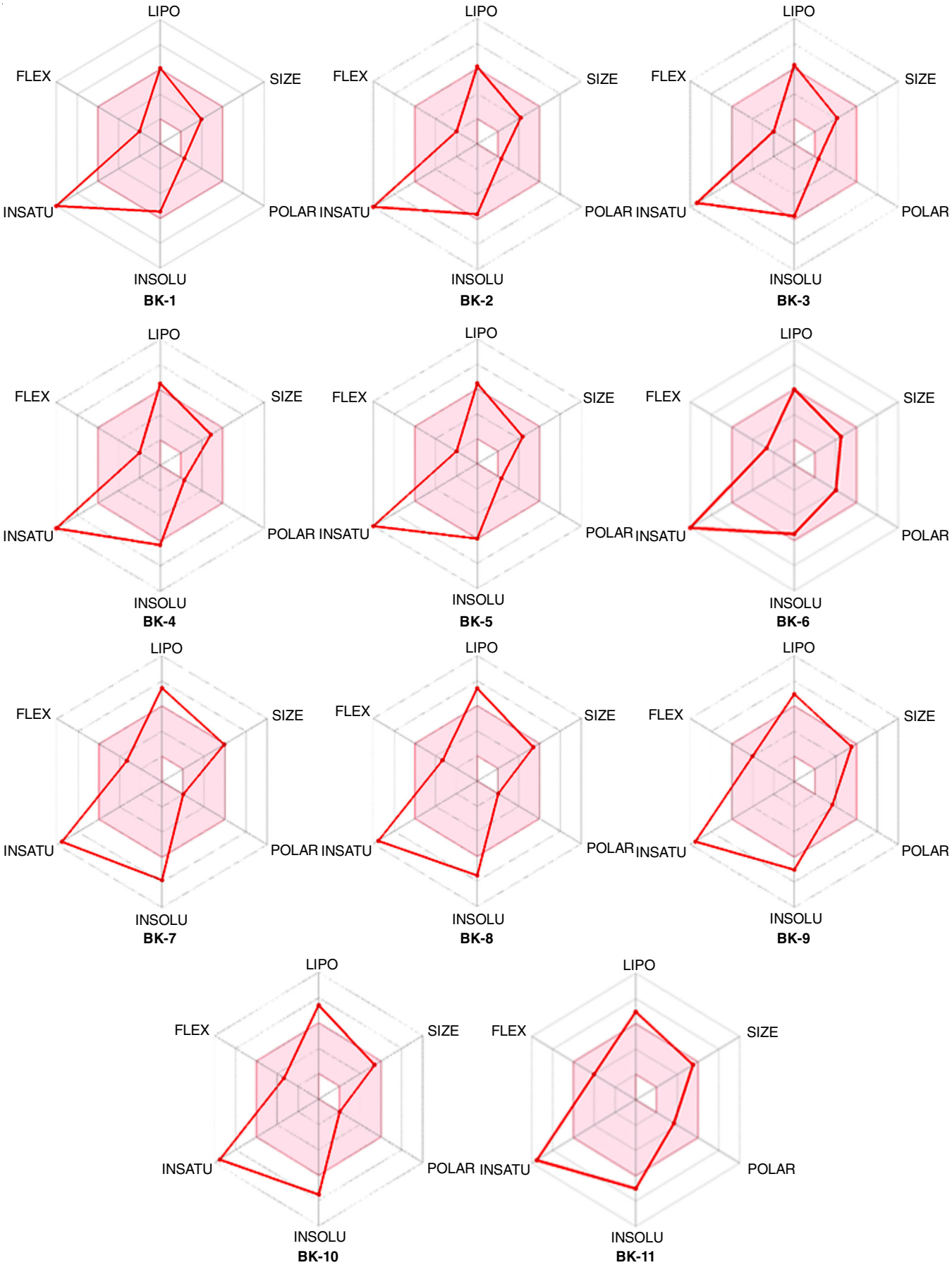

Fig. 1. Physico-chemical parameters space for oral bioavailability of **BK-1** to **BK-11**

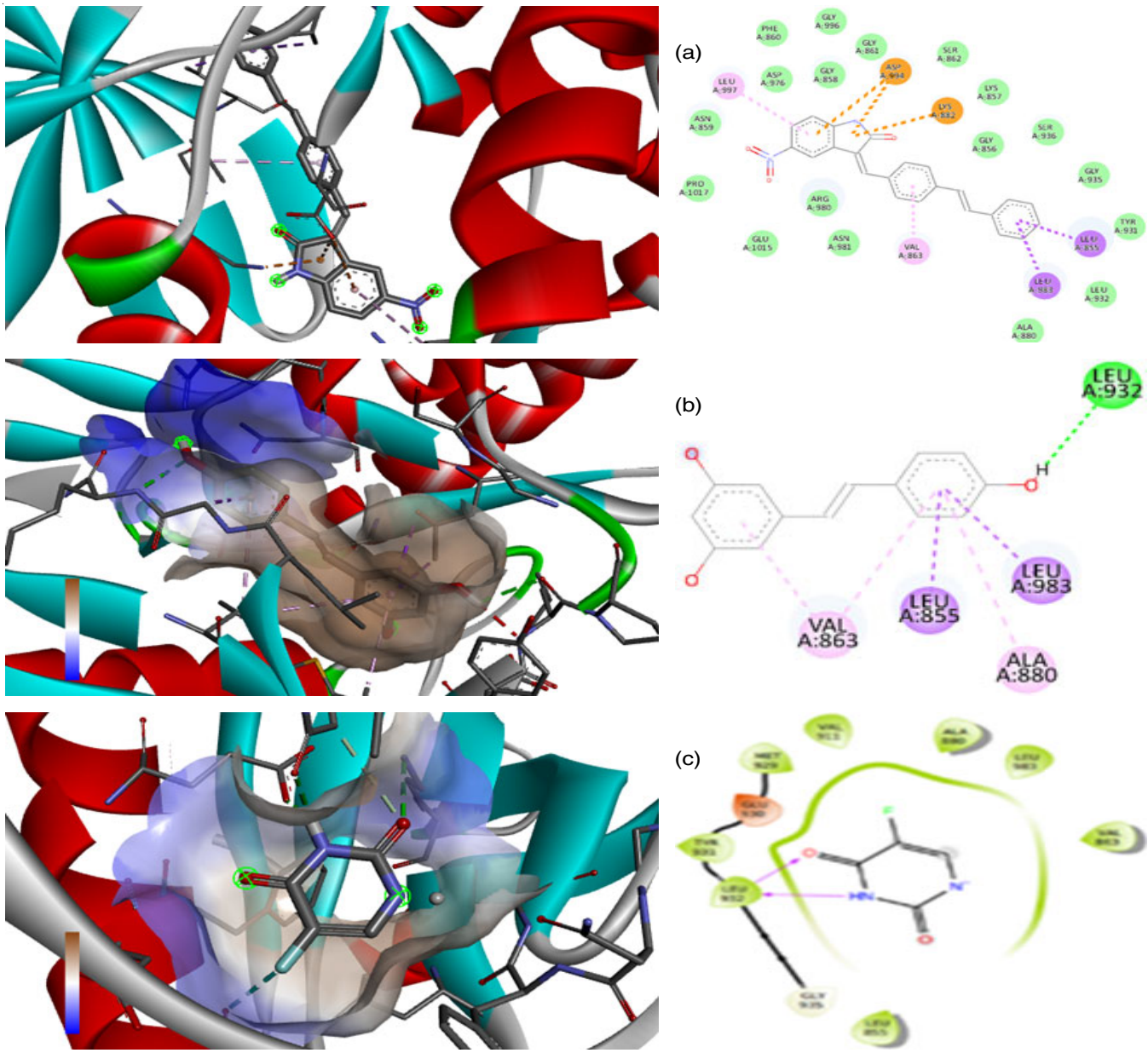

Fig. 2. Interaction of compound **BK-6** (a), RSV (b) and 5FU (c) with 4Z32 protein (JAK2 receptor)

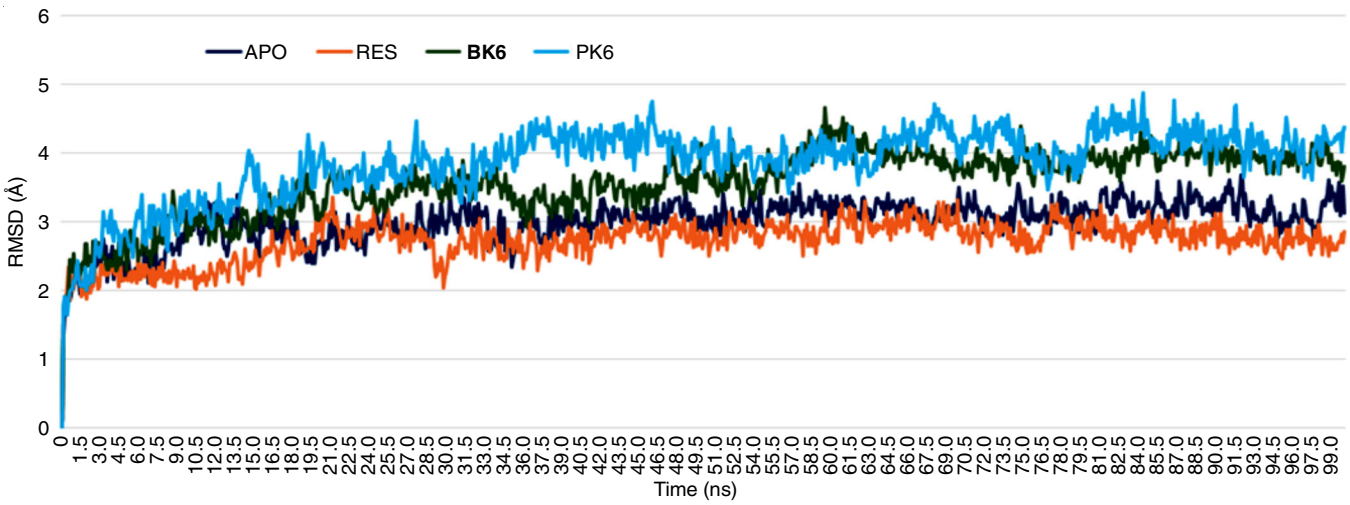

Fig. 3. Root mean square deviation (RMSD) plot

TABLE-3
PHYSICO-CHEMICAL AND PHARMACOKINETIC PROPERTIES OF
(*Z*)-3-(4-((*E*)-STYRYL)BENZYLIDENE)INDOLIN-2-ONE (**BK-1** TO **BK-11**)

Compd.	Physico-chemical properties							Lipophilicity					
	MW	Csp3	RB	HBA	HBD	MR	TPSA	Ilogp	XLOGP3	WLOGP	MLOGP	Silicos-IT	Consensus
BK-1	323.39	0	3	1	1	107.51	29.1	3.35	5.17	4.45	4.35	5.6	4.58
BK-2	341.38	0	3	2	1	107.47	29.1	3.42	5.27	5.01	4.72	6	4.89
BK-3	337.41	0.04	3	1	1	112.47	29.1	3.58	5.53	4.76	4.56	6.11	4.91
BK-4	402.28	0	3	1	1	115.21	29.1	3.62	5.86	5.21	4.93	6.26	5.18
BK-5	357.83	0	3	1	1	112.52	29.1	3.53	5.79	5.1	4.83	6.22	5.1
BK-6	368.38	0	4	3	1	116.33	74.92	2.85	4.99	4.36	3.27	3.4	3.78
BK-7	492.41	0.03	5	1	0	144.6	20.31	4.65	7.53	6.85	6.1	7.65	6.56
BK-8	447.95	0.03	5	1	0	141.91	20.31	4.61	7.47	6.74	6.01	7.62	6.49
BK-9	458.51	0.03	6	3	0	145.72	66.13	3.93	6.67	5.99	4.48	4.8	5.17
BK-10	447.95	0.03	5	1	0	141.91	20.31	4.6	7.47	6.74	6.01	7.62	6.49
BK-11	458.51	0.03	6	3	0	145.72	66.13	4.02	6.67	5.99	4.48	4.8	5.19

Compd.	Drug likeliness					Water solubility		Pharmacokinetics	
	Lipinski	Ghose	Veber	Egan	Muegge	ESOL Log S	ESOL Class	log Kp	F
BK-1	1	0	0	0	1	-5.44	Moderate soluble	-4.6	0.55
BK-2	1	0	0	0	1	-5.59	Moderately soluble	-4.64	0.55
BK-3	1	0	0	0	1	-5.73	Moderately soluble	-4.43	0.55
BK-4	1	0	0	0	1	-6.34	Poorly soluble	-4.59	0.55
BK-5	1	0	0	0	1	-6.02	Poorly soluble	-4.37	0.55
BK-6	0	0	0	0	0	-5.48	Moderately soluble	-5	0.55
BK-7	1	3	0	1	1	-7.84	Poorly soluble	-3.96	0.55
BK-8	1	2	0	1	1	-7.53	Poorly soluble	-3.73	0.55
BK-9	1	2	0	1	1	-7	Poorly soluble	-4.36	0.55
BK-10	1	2	0	1	1	-7.53	Poorly soluble	-3.73	0.55
BK-11	1	2	0	1	1	-7	Poorly soluble	-4.36	0.55

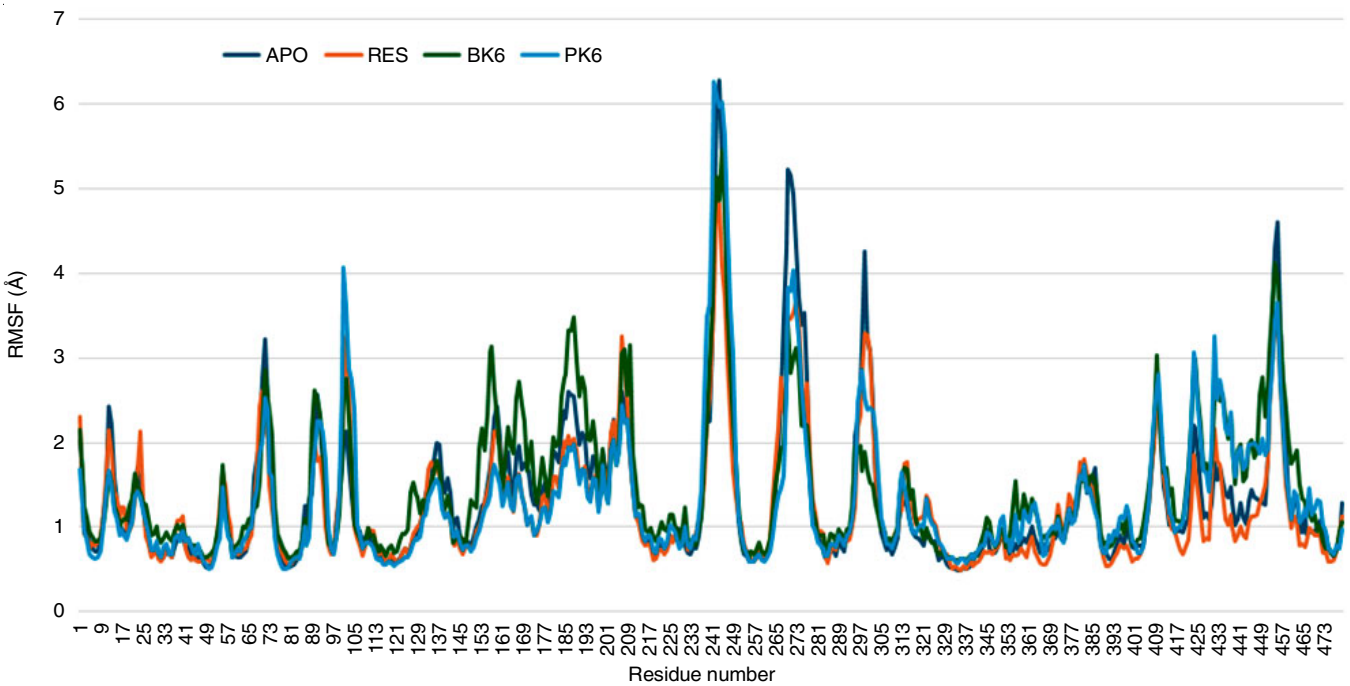

Fig. 4. Root mean square fluctuation (RMSF) plot

the analogues, compound **BK-6** emerged as the most potent, with IC_{50} values of 48 µM, 64 µM and 57 µM against MCF-7, HCT-116 and HeLa cell lines, respectively. Furthermore, *in silico* ADME analysis showed that compound **BK-6** violated none of the Lipinski, Ghose, Veber, Egan or Muegge rules and exhibited moderate water solubility. These results suggest that indole-linked stilbenes possess promising cytotoxic activity against various cancer cell lines. Therefore, this study paves the way for future investigations aimed at developing novel therapeutic strategies for cancer treatment.

TABLE-4
BINDING AFFINITY (Kcal/mol) OF (Z)-3-(4-((*E*)-STYRYL) BENZYLIDENE)INDOLIN-2-ONES (**BK-1** TO **BK-11**), RESVERATROL AND 5-FU WITH PROTEIN 4Z32 (JAK2 RECEPTOR)

Code	Docking score	Code	Docking score
BK-1	-7.3	**BK-8**	-6.1
BK-2	-7.3	**BK-9**	-4.1
BK-3	-7.6	**BK-10**	-6.9
BK-4	-7.8	**BL-11**	-4.4
BK-5	-7.3	RSV	-7.8
BK-6	-7.8	5FU	-6.4
BK-7	-5.8		

ACKNOWLEDGEMENTS

The authors thank Agilent Technologies, Bengaluru (India) for LC-MS and NMR Research Centre-Indian Institute of Science, Bengaluru (India) for ^{1}H & ^{13}C NMR spectral data and KLE College of Pharmacy, Bengaluru for the support to complete the work.

CONFLICT OF INTEREST

The authors declare that there is no conflict of interests regarding the publication of this article.

REFERENCES

1. F. Bray, M. Laversanne, J. Ferlay, R.L. Siegel, I. Soerjomataram, H. Sung and A. Jemal, *CA Cancer J. Clin*., **74**, 229 (2024); https://doi.org/10.3322/caac.21834
2. R.L. Siegel, K.D. Miller and A. Jemal, *CA Cancer J. Clin.*, **68**, 7 (2018); https://doi.org/10.3322/caac.21442
3. S.C. Gupta, R. Kannappan, S. Reuter, J.H. Kim and B.B. Aggarwal, *Ann. N. Y. Acad. Sci.*, **1215**, 150 (2011); https://doi.org/10.1111/j.1749-6632.2010.05852.x
4. J. Tian, L. Jin, H. Liu and Z. Hua, *Front. Pharmacol.*, **14**, 1326682 (2023); https://doi.org/10.3389/fphar.2023.1326682
5. M.K. Konstantinos and A.H. Serkos, *Curr. Org. Chem.*, **16**, 335 (2012); https://doi.org/10.2174/138527212799499886
6. F. Borys, P. Tobiasz, M. Potera³a, H. Fabczak, H. Krawczyk and E. Joachimiak, *Molecules*, **28**, 3558 (2023); https://doi.org/10.3390/molecules28083558
7. K. Hagiwara, N. Kosaka, Y. Yoshioka, R. Takahashi, F. Takeshita and T. Ochiya, *Sci. Rep.*, **2**, 314 (2012); https://doi.org/10.1038/srep00314
8. P. Pecyna, J. Wargula, M. Murias and M. Kucinska, *Biomolecules*, **10**, 1111 (2020); https://doi.org/10.3390/biom10081111
9. A. Kumari and R.K. Singh, *Bioorg. Chem.*, **89**, 103021 (2019); https://doi.org/10.1016/j.bioorg.2019.103021.
10. S. Siddique, K.R. Ahmad, S.K. Nawaz, A.R. Raza, S.N. Ahmad, R. Ali, I. Inayat, S. Suleman, M.A. Kanwal and M. Usman., *Sci. Rep.*, **13**, 8639 (2023); https://doi.org/10.1038/s41598-023-35640-4
11. A.A. Ahmad, K. Hussain, M.R. Shah, S.M. Ashhad Halimi, F. Rabbi, Z. Ahmad, I. Khan, A. Rauf, A. Alshammari, M. Alharbi and H.A. Rasul Suleria, *ACS Omega*, **8**, 30048 (2023); https://doi.org/10.1021/acsomega.3c02033
12. T. Blazevic, E.H. Heiss, A.G. Atanasov, J.M. Breuss, V.M. Dirsch and P. Uhrin, *Evid. Based Complement. Alternat. Med.*, **2015**, 654098 (2015); https://doi.org/10.1155/2015/654098
13. L. Liu, Y.-Y. Chen, X.-J. Qin, B. Wang, Q. Jin, Y.-P. Liu and X.-D. Luo, *Fitoterapia*, **105**, 160 (2015); https://doi.org/10.1016/j.fitote.2015.06.019
14. A. Sharma, P. Verma, A. Mathur and A.K. Mathur, *Protoplasma*, **255**, 1281 (2018); https://doi.org/10.1007/s00709-018-1233-1
15. V. De Luca and B. St Pierre, *Trends Plant Sci.*, **5**, 168 (2000); https://doi.org/10.1016/S1360-1385(00)01575-2
16. D. Kumar, S. Sharma, S. Kalra, G. Singh, V. Monga and B. Kumar, *Curr. Drug Targets*, **21**, 864 (2020); https://doi.org/10.2174/1389450121666200310115327
17. N.K. Kaushik, N. Kaushik, P. Attri, N. Kumar, C.H. Kim, A.K. Verma and E.H. Choi, *Molecules*, **18**, 6620 (2013); https://doi.org/10.3390/molecules18066620
18. P.V. Thanikachalam, R.K. Maurya, V. Garg and V. Monga, *Eur. J. Med. Chem.*, **180**, 562 (2019); https://doi.org/10.1016/j.ejmech.2019.07.019.
19. A. Das, S. Kumar, L. Persoons, D. Daelemans, D. Schols, H. Alici, H. Tahtaci and S.S. Karki, *Heliyon*, **7**, e05893 (2021); https://doi.org/10.1016/j.heliyon.2020.e05893
20. E. Thomas, V. Gopalakrishnan, M. Hegde, S. Kumar, S.S. Karki, S.C. Raghavan and B. Choudhary, *Sci. Rep.*, **6**, 34653 (2016); https://doi.org/10.1038/srep34653
21. D. Iyer, S.V. Vartak, A. Mishra, G. Goldsmith, S. Kumar, M. Srivastava, M. Hegde, V. Gopalakrishnan, M. Glenn, M. Velusamy, B. Choudhary, N. Kalakonda, S.S. Karki, A. Surolia and S.C. Raghavan, *FEBS J.*, **283**, 3408 (2016); https://doi.org/10.1111/febs.13815
22. F.J. Solis and R.J.B. Wets, *Math. Oper. Res.*, **6**, 19 (1981); https://doi.org/10.1287/moor.6.1.19
23. R. Huey, G.M. Morris, A.J. Olson and D.S. Goodsell, *J. Comput. Chem.*, **28**, 1145 (2007); https://doi.org/10.1002/jcc.20634
24. BIOVIA Discovery Studio, Discovery Studio Modeling Environment, Dassault Systemes Release, San Diego (2017).
25. M.D. Hanwell, D.E. Curtis, D.C. Lonie, T. Vandermeersch, E. Zurek and G.R. Hutchison, *J. Cheminform.*, **4**, 17 (2012); https://doi.org/10.1186/1758-2946-4-17
26. S. Dallakyan and A.J. Olson, *Methods Mol. Biol.*, **1263**, 243 (2015); https://doi.org/10.1007/978-1-4939-2269-7_19
27. A. Daina, O. Michielin and V. Zoete, *Sci. Rep.*, **7**, 42717 (2017); https://doi.org/10.1038/srep42717
28. A. Daina, O. Michielin and V. Zoete, *J. Chem. Inf. Model.*, **54**, 3284 (2014); https://doi.org/10.1021/ci500467k
29. D. Yevale, N. Teraiya, T. Lalwani, M. Dalasaniya, K. Kapadiya, R.K. Ameta, C.B. Sangani and Y.-T. Duan, *Bioorg. Chem.*, **147**, 107323 (2024); https://doi.org/10.1016/j.bioorg.2024.107323